Biometric Verification by Fusing Hand Geometry and Palmprint Features for Personal Authentication

Wen-Shiung Chen
VIPCCL, Dept. of Electrical Engineering, National Chi Nan University, Nan-Tou, Taiwan

Lili Hsieh
Dept. of Information Management, Hsiuping University of Science and Technology, Taichung, Taiwan

Yao-Shan Chiang
VIPCCL, Dept. of Electrical Engineering, National Chi Nan University, Nan-Tou, Taiwan

Abstract – This paper presents a biometric recognition system with fusion of hand geometry and palmprint of a human hand based on wavelet transform and statistical moments for personal authentication. The proposed system consists mainly of four modules: image acquisition, image preprocessing, feature extraction, and recognition modules. Image preprocessing module uses some image processing algorithms to localize the region of interest of palmprint and hand geometry from input images. The feature extraction module adopts the gradient direction (i.e., angle) and quadratic spline function of wavelet transform as the discriminating texture features in palmprint, and the statistical moments calculated from hand geometry. The system generates the palmprint feature codes using a coding technique: binary gray encoding. Experimental results show that the proposed recognition system has an encouraging performance on our own hands database. The recognition rates up to 94.17%, 95.50%, 96.67%, and 98.33%, respectively, using different feature extraction methods may be achieved.

Index Terms – Biometrics, Biometric Verification, Hand Geometry, Palmprint, Wavelet Transform, Moment.

1. INTRODUCTION

Reliability in the personal authentication (or identity authentication) is critical to a wide range of applications in the networked society. *Biometrics* [1][2] refers to automatic identity authentication of a person on a basis of one's unique physiological or behavioral characteristics, and is inherently more suitable for discriminating between an authorized person and an impostor than traditional methods. Under such circumstances, biometrics offers the most secure means to automatically identify individuals without requiring them to carry ID cards or memorize passwords. Typically, these automatic biometric-based authentication systems are classified into two major categories: *one-to-one* (or *verification*) and *one-to-many* (or *identification*) [1]. To date, many biometric features, including fingerprint, hand geometry or palmprint, face, handwritten signature, voice, DNA, retina, and iris, have been studied and applied to the authentication of individuals [1][2].

Most of the existing techniques have limited capabilities in recognizing relatively complex features in realistic situations. Compared with the other physical characteristics, although a human hand-based biometric authentication system is usually considered to achieve medium security, it has several advantages: (i) non-intrusiveness, (ii) stable line features, (iii) low code size, (iv) low mechanism cost, (v) low computational cost, and (vi) high user acceptance. Besides, the rich texture information of palmprint offers one of the powerful means in biometric authentication. From all these advantages, in this paper we investigate and design a biometric recognition system by fusing the features of hand geometry and palmprint.

2. PRIOR WORK

In human hands, two kinds of biometric features can be extracted from the low-resolution images; (i) hand geometry (or shape) features, which are composed of area/size of palm, length and width of fingers, and (ii) palmprint features, which include principal lines, wrinkles, minutiae, delta points, *etc*. Hand geometry-based authentication techniques are very effective for various reasons and have been commercialized for almost three decades. However, in the literature, their technical articles are still rare and the available information is based mostly on patents. The work on hand geometry recognition done by Golfarelli *et al*. [3] extracts 17 hand geometry features to verify the personal identity. Jain *et al*. proposed a prototype hand geometry-based verification system in which some typical features, such as length and width of the fingers, aspect ratio of the palm or fingers, thickness of the hand, etc., are extracted along the 16 axes [4]. Jain *et al*. [5] also used the deformable matching techniques to verify the individuals via the hand geometry. The hand geometry of a test sample is aligned with that in the database, and a defined distance is calculated for evaluation of similarity. Sanchez-Reillo *et al*. introduced an identification system that 31 features are extracted (including 21 widths, 3 heights, 4 deviations and 3 angles). Some different pattern

recognition techniques, such as Gaussian Mixture Models (GMMs) and Radial Basis Function Neural Networks (RBF), have been tested [6][7]. Wong and Shi [8] presented a peg-free hand geometry system by using a flatbed optical scanner for hand image capturing and by extracting significant geometrical landmarks of a hand to align the hands to a certain direction. In [9], Zheng, Boult and Wang presented a projective invariant hand-geometry approach based on 16 features and cross-ratios computed from subsets of 5 points. Zunkel [10] introduced a commercial product of hand geometry-based recognition and applied it to many access control systems. Several patents [11][12][13] for hand geometry identification have been designed.

On the other hand, palmprint recognition has attracted an increasing amount of attention from researchers recently. A palm, the inner surface of a human hand between the wrist and the fingers, is composed of three parts: the finger-root region, inside region and outside region. Palmprint recognition is a novel biometric method to extract palmprint features that can discriminate an individual from the other. Generally, there are three types of features embedded in palmprint: *structural features*, *statistical features* and *algebraic features*. Basically, structural features, such as principal lines, wrinkles, delta points, minutiae, features points, interesting points and etc., can characterize a palm exactly, but are difficult to be extracted and represented; while statistical features can be extracted by using appropriate transforms and represented easily, but are unable to reflect the structural information of a palmprint. Algebraic features, which represent intrinsic attributions of a palm, can be extracted based on various algebraic transform operations or matrix decompositions. There are many approaches for palmprint recognition in various literatures.

The structural features can be extracted and represented by using pattern-based (or geometry-based) approach. In articles [14][15] by Su and Zhang, there are three principal lines made by flexing the hand and wrist in the palm, which are usually defined as life line, heart line, and head line. Duta *et al*. [16] presented an off-line palmprint identification system which processes low-resolution images captured by a low cost and non-intrusive device to extract stable structural features. Han *et al*. [17] proposed a scanner-based personal authentication system using palmprint features. It extracts features using Sobel and morphological operations, template-matching, and the backpropagation neural network to measure the similarity in the verification stage.

The statistical features can be easily extracted and represented by means of statistics-based approach. In [18], Zhang simply used the texture energy to represent the palmprint features. Pang *et al*. [19][20] introduced a palmprint verification by utilizing three well-known orthogonal moments such as Zernike moments, pseudo Zernike moments and Legendre moments. Some different statistics-based methods may refer to [21][22][23]. Wu, Wang and Zhang [22] borrowed the idea of an efficient Chinese character recognition method, the directional element feature, to define a novel palmprint feature, named the fuzzy directional element energy feature (FDEEF) which is a statistical feature containing some line structural information about palmprints. Jain, Pradeep, and Balasubramanian [23] proposed a new approach to the palmprint verification based on nearest neighbor vector (NNV).

Those algebraic features can be extracted and represented with either transform-based approach or projection-based approach. The transform-based approaches always transform the original data into another domain in which the features are then easily extracted and represented. Among the works that appear in the literature are Fourier transform [24], Wavelet transform [25] and 2-D Gabor filter [26][27]. Li, Zhang and Xu [24] proposed a new feature extraction method by converting a palmprint image from a spatial domain to a frequency domain using Fourier Transform. The features extracted in the frequency domain are used as indexes to the palmprint templates in the database and the searching process for the best match is conducted by a layered fashion. The experimental results show that palmprint identification based on feature extraction in the frequency domain is effective in terms of accuracy and efficiency. A palmprint recognition system based on wavelet-based features was proposed by Kumar and Shen [25]. Zhang *et al*. [26][27] applied a texture-based feature extraction technique to palmprint authentication. A 2-D Gabor filter is used to obtain texture information and two images are compared in terms of their Hamming distance.

Alternatively, the projection-based approaches always project the original higher-dimensional data into a lower-dimensional space in which the features are then effectively extracted and represented. Liu *et al*. [28] designed a method to extract the algebraic features. In [29], Fisher's linear discriminant (FLD) is an efficient approach to extract the algebraic features that have strong discriminability. Borrowing the concept of eigenface and Fisherface from face recognition, D. Zhang *et al*. [30][31] also applied eigenspace technology and a linear projection based on Fisher's linear discriminant technology to palmprint authentication to propose two approaches, namely eigenpalm [30] and Fisherpalm [31]. Connie *et al*. [32] applied two well-known linear projection techniques, namely Principal Component Analysis (PCA) and Independent Component Analysis (ICA) to extract the palmprint texture features. A commercial product system for automatic palmprint Identification has been developed by NEC company [33]. Furthermore, some bimodal biometric recognition systems which integrate the features of both hand-shape and palmprint have been introduced [34][35].

3. SYSTEM ARCHITECTURE AND PRE-PROCESSING

3.1 System Overview

The proposed framework consists of four modules: image acquisition, image pre-processing, feature extraction and recognition modules, as shown in Figure 1. The entire system diagram is briefly described as follows. First, the palmprint and hand geometry image acquisition module (PHIA module) uses a CCD-based digital camera to capture the hand images, then the palmprint and hand geometry image pre-processing module (PHIP module) employs some image processing algorithms to demarcate the region of interest (R.O.I.; i.e., palmprint zone) from an input image containing a hand. This module performs three major tasks, including palmprint and hand geometry pre-processing, segmentation of R.O.I of palmprint [17], and enhancement for the input hand image. Next, the feature extraction module (PHFE module) performs a 2-D wavelet transform, computes the gradient direction features and statistical moments, computes the invariant moments, and applies proper coding methods on these features to generate a palmprint code and a hand geometry feature vector. Finally, the pattern recognition module (PHPR module) employs a minimum distance classifier according to Euclidean distance and Hamming distance metric to recognize the hand pattern by comparing the palmprint code and feature vector with the enrolled data in the PPC & SMV database.

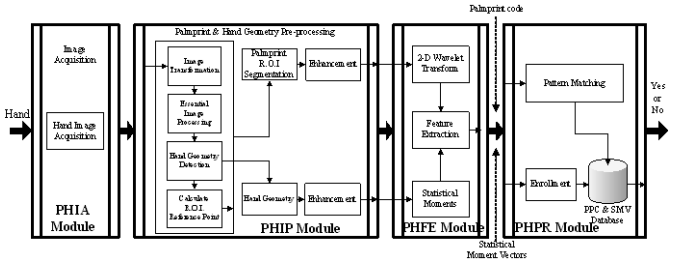

Figure 1 System diagram of the proposed palmprint and hand geometry-based biometric recognition system.

3.2 Image Acquisition Module

The proposed on-line hand-geometry and palmprint recognition system expects to provide a simple, low-cost, non-contact, comfortable and user-friendly acquisition mechanism. The acquisition mechanism for hand image is shown in Figure 2. In order to make the system suitable for any applications and environments, we design a flatbed-less and peg-free mechanism which adopts a capturing device (Sony DSC-F717 CCD-based digital camera with a resolution of 1,280×960 pixels without flashlight) to acquire high quality images. In addition, two 3U 23-watt lights are also arranged in appropriate positions (see Figure 2) to capture a good quality hand image in the proposed system. Unlike other bimodal biometric systems in which the different modalities may be acquired using different sensors, undergoing the inconvenience to the users and more system cost, the proposed mechanism can acquire the hand-shape and palmprint features on-line from the same image simultaneously by simply using a digital camera.

Figure 2 The palmprint and hand geometry image acquisition module (PHIA module).

3.3 Pre-processing Module

Image pre-processing is usually the first and essential step in pattern recognition. In the proposed approach, two different algorithms are designed for palmprint and hand geometry, respectively, in the pre-processing module. For palmprint, the pre-processing module includes seven steps: file transformation, color-to-gray transformation, gray-to-binary transformation, edge detection, R.O.I. reference points searching, R.O.I. defining and segmentation [17], and enhancement, as shown in Figure 3(a). On the other hand, for the hand geometry the pre-processing module has an enhancement step, as shown in Figure 3(b). In the following, we will describe the details of each step.

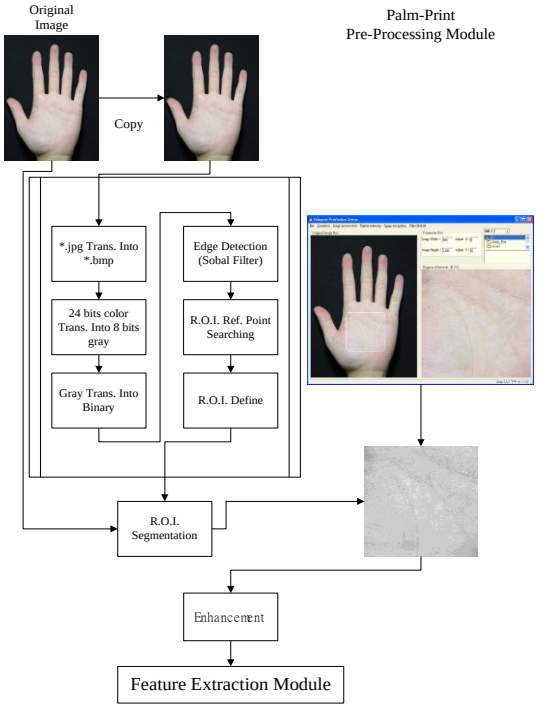

(a) Palmprint.

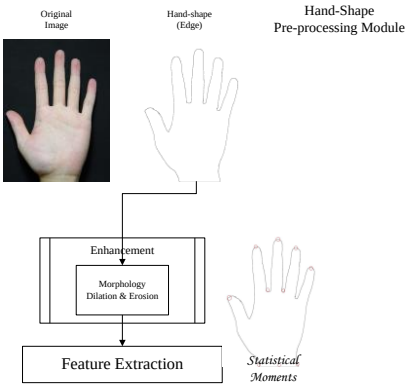

(b) Hand geometry.

Figure 3 The flowchart of pre-processing module.

1). Pre-processing for Palmprint

Step1: *File conversion*. In the acquisition module, the capturing device (i.e., digital camera) stores the input hand image in the *.jpg format. Therefore, we need to converse it into *.bmp format for the following processes.

Step2: *Color-to-gray transformation* [36]. Since gray-level image is adequate for hand shape segmentation process, we need to convert color image to gray-level image by using the following conversion formula,

$$Y=0.299\times R+0.587\times G+0.114\times B. \quad (1)$$

Step3: *Gray-to-binary transformation*. The image threshold operation binarizes the gray image to obtain the binary hand geometry images. In this step, the histogram of gray images is analyzed and shown in Figure 4. In our system we choose a fixed threshold of 75, as show in Figure 4.

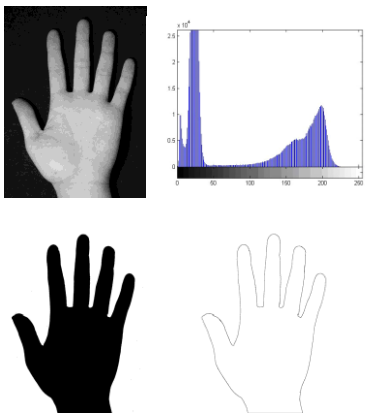

Figure 4 Four transformation steps for the hand images.

Step4: *Edge detection*. In this step, we trace the binary image to obtain the contours of hand geometry using four-direction Sobel filter, as shown in Figure 4.

Step5: *R.O.I. reference points searching*. According to the result generated in step 4, the location of R.O.I. is determined from V_L, V_R, and P_3 by using a simple geometrical formula. First, we choose the two points, V_L and V_R, as the base points for defining the R.O.I. Next, the middle point P_a is obtained from the points V_L and V_R. The principal axis $\overline{P_3P_a}$ is then easily obtained, which is the center line of middle finger perpendicular bisector line $\overline{V_LV_R}$. The principal axis $\overline{P_3P_a}$ is then extended to the point P_b, where $\overline{|P_aP_b|}=0.8\times\overline{|V_LV_R|}$.

Step6: *R.O.I. defining and segmentation*. From the point P_b, we obtain two perpendicular bisector lines, denoted as $\overline{P_{el}P_b}=\overline{P_bP_{er}}$, whose lengths are both equal to 175 pixels. Accordingly, the square region of size 350×350 is defined and segmented as the R.O.I., as shown in Figure 5.

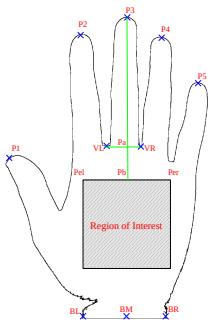

Figure 5 The region of interest of palmprint.

Step7: *Enhancement*. In this step, we use the histogram equalization technique to enhance the R.O.I. image of palmprint.

2). Pre-processing for Hand Geometry

After performing step 4, the shape of the hand is obtained. For hand geometry the pre-processing module adopts some simple morphological techniques to enhance the image for the following feature extraction module, as shown in Figure 3(b).

4. THE PROPOSED RECOGNITION TECHNIQUES

4.1 Wavelet Transform-based Edge Detection

Wavelet transform (WT) has been widely used in the last few years to solve the intrinsic redundancies that appear in a multi-scale analysis [38]-[41]. In this paper, we have analyzed the different scale information given by the wavelet transform to acquire the abundant edge information in the iris image $f(x, y)$. A multi-scale version of this edge detector is designed by

smoothing the surface with a convolution kernel $\theta(x, y)$ that is dilated. For the scale 2^j, we denote

$$\theta_{2^j}(x,y) = 2^{-j}\theta(2^{-j}x, 2^{-j}y)$$

and

$$\bar{\theta}_{2^j}(x,y) = \theta_{2^j}(-x,-y).$$

In the two directions (x-direction and y-direction), the dyadic wavelet transform of $f \in L^2(R)$ at (u, v) is

$$W_{2^j}^k f(u,v) = \left\langle f(x,y), \psi_{2^j}^k(x-u, y-v) \right\rangle. \quad (2)$$

We thus derive from (2) that the wavelet transform components are proportional to the coordinates of the gradient vector of f smoothed by $\bar{\theta}_{2^j}$:

$$\begin{pmatrix} W_{2^j}^1 f(u,v) \\ W_{2^j}^2 f(u,v) \end{pmatrix} = 2^j \begin{pmatrix} \frac{\partial}{\partial x}\left(f * \bar{\theta}_{2^j}\right)(u,v) \\ \frac{\partial}{\partial y}\left(f * \bar{\theta}_{2^j}\right)(u,v) \end{pmatrix} = 2^j \vec{\nabla}\left(f * \bar{\theta}_{2^j}\right)(u,v) \quad (3)$$

The modulus of this gradient vector is proportional to the wavelet transform modulus

$$M_{2^j} f(u,v) = \sqrt{\left|W_{2^j}^1 f(u,v)\right|^2 + \left|W_{2^j}^2 f(u,v)\right|^2} \quad (4)$$

Let $A_{2^j} f(u, v)$ be the angle of the gradient direction (wavelet transform) vector (Eq. (3)) in the plane (x, y). We obtain

$$A_{2^j} f(u,v) = \tan^{-1}\left(\frac{W_{2^j}^2 f(u,v)}{W_{2^j}^1 f(u,v)}\right). \quad (5)$$

The unit vector $\vec{n}_j(u,v) = \left(\cos A_{2^j} f(u,v), \sin A_{2^j} f(u,v)\right)$ is colinear to $\vec{\nabla}\left(f * \bar{\theta}_{2^j}\right)(u,v)$. An edge point at the scale 2^j is a point γ such that $M_{2^j} f(u, v)$ is locally maximum at $(u=u_\gamma, v=v_\gamma)$ when $\left(u = u + \lambda h_j(u_\gamma), v = v + \lambda h_j(v_\gamma)\right)$ is small enough for $|\lambda|$. These points are also called the wavelet transform modulus maxima. The criterion for detecting edge is summarized as follows:

Step1: Compute the x-direction wavelet transform (i.e., $W_{2^j}^1 f(u,v)$) and the y-direction wavelet transform (i.e., $W_{2^j}^2 f(u,v)$).

Step2: Compute the modulus (i.e., $M_{2^j} f(u,v)$) and the gradient direction (i.e., $A_{2^j} f(u,v)$) in the wavelet transform.

Step3: Set a threshold T. The pixel point (x, y) is an edge point if (i) $|M_{2^j} f(u,v)| \geq T$ and (ii) $M_{2^j} f(u,v)$ is the local maximum along the direction of $A_{2^j} f(u,v)$.

4.2 Feature Extraction with Wavelet Transform

The edge structures in iris images are often the most important features for pattern recognition and clear at a variety of scales. To extract the spatial details of an image, it is advantageous to make use of a multi-scale representation. The wavelet transform is capable of focusing on localized structures with a zooming procedure that progressively reduces the scale parameter. In the paper, we extract the angle of the gradient direction (Eq. (5)) of the wavelet transform as the iris feature and encode it efficiently.

First, we apply wavelet transform on the iris image and compute the angle of the gradient direction at a specific scale. In this paper, we use quadratic spline function (Figure 6(b)) as the wavelet function, which is the derivative of the cubic spline function shown in Figure 6(a) [39][40]. The scaling function (smoothing function) is defined as

$$\theta(x) = \begin{cases} 8\left(x^3 - x^2\right) + \frac{4}{3} & 0 \leq |x| \leq \frac{1}{2} \\ -\frac{8}{3}(x-1)^3 & \frac{1}{2} < |x| \leq 1 \\ 0 & |x| > 1 \end{cases}. \quad (6)$$

And the wavelet function is easily obtained as

$$\psi(x) = \begin{cases} 8\left(3x^2 - 2x\right) & 0 \leq x \leq \frac{1}{2} \\ -8(x-1)^2 & \frac{1}{2} < x \leq 1 \\ 0 & x > 1 \end{cases}. \quad (7)$$

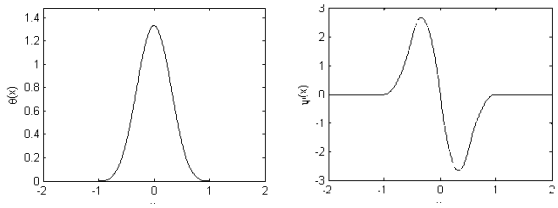

(a) (b)

Figure 6 (a) Cubic spline function. (b) Quadratic spline wavelet function.

Edge points are distributed along curves that often correspond to the boundary of important structures. Individual wavelet modulus maxima are chained together to form a curve that follows an edge. At any location, the tangent of the edge curve is approximated by computing the tangent of the angle of the gradient direction [37]. Thus, we select the angle of the gradient direction as the iris feature for recognition. It is advantageous because the gradient direction will not be affected by contrast and illumination of the input images. Figure 7 shows the iris images of x-direction wavelet

transform $W_{2^j}^1 f(u,v)$, y-direction wavelet transform $W_{2^j}^2 f(u,v)$ obtained by quadratic spline wavelet transform for the scales j= 1, 2, 3. Since singularities and irreguar structures in palmprint images often carry essential information, we adopt two different representations, including 2-D Gray encoding and 1-D delta modulation encoding, based on the edge detection with wavelet transform in this module to extract and encode the features from a human palmprint image.

(a)

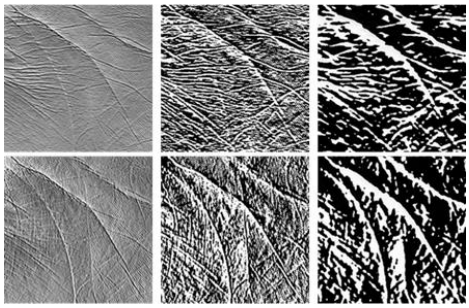

(b) upper (c) lower

Figure 7 Palmprint images obtained by quadratic spline wavelet transform (j= 1, 2, 3, from left to right): (a) original image, (b) x-direction WT, $W_{2^j}^1 f(u,v)$, (c) y-direction WT, $W_{2^j}^2 f(u,v)$.

4.3 Feature Extraction with Statistical Moments

For a 2-D continuous function $f(x, y)$, the moment of order $(p + q)$ is defined as

$$m_{pq} = \int_{-\infty}^{\infty}\int_{-\infty}^{\infty} x^p y^q f(x,y)dxdy \text{ , for } p,q = 0,1,2,3\ldots.$$

A uniqueness theorem states that if $f(x, y)$ is piecewise continuous and has nonzero values only in a finite part if the xy -plane, moments of all order exits, and the moment sequence (m_{pq}) is uniquely determined by $f(x, y)$. Conversely, (m_{pq}) uniquely determines $f(x, y)$. The central moments are defined as

$$\mu_{pq} = \int_{-\infty}^{\infty}\int_{-\infty}^{\infty} (x-\bar{x})^p (y-\bar{y})^q f(x,y)dxdy, \quad (8)$$

where

$$\bar{x} = \frac{m_{10}}{m_{00}} \text{ and } \bar{y} = \frac{m_{10}}{m_{00}}.$$

If $f(x, y)$ is a digital image, then Eq. (8) becomes

$$\mu_{pq} = \sum_x \sum_y (x-\bar{x})^p (y-\bar{y})^q f(x,y).$$

The central moments [36] of order up to 3 are

$$\mu_{00} = m_{00}, \qquad \mu_{11} = m_{11} - \bar{y}m_{10},$$

$$\mu_{10} = 0, \qquad \mu_{30} = m_{30} - 3\bar{x}m_{20} + 2\bar{x}^2 m_{10},$$

$$\mu_{01} = 0, \qquad \mu_{12} = m_{12} - 2\bar{y}m_{11} - \bar{x}m_{02} + 2\bar{y}^2 m_{10},$$

$$\mu_{20} = m_{20} - \bar{x}m_{10}, \quad \mu_{21} = m_{21} - 2\bar{x}m_{11} - \bar{y}m_{20} + 2\bar{x}^2 m_{01},$$

$$\mu_{02} = m_{02} - \bar{y}m_{01}, \quad \mu_{03} = m_{03} - 3\bar{y}m_{02} + 2\bar{y}^2 m_{01}.$$

The normalized central moments, denoted η_{pq}, are defined as

$$\eta_{pq} = \frac{\mu_{pq}}{\gamma_{00}^{\gamma}} \text{ , where } \gamma = \frac{p+q}{2} + 1 \text{ , for } p+q = 2,3,\ldots.$$

A set of seven invariant moments can be derived from the second and third moments [36].

$$\phi_1 = \eta_{20} + \eta_{02}, \quad \phi_2 = (\eta_{20} - \eta_{02})^2 + 4\eta_{11}^2,$$

$$\phi_3 = (\eta_{30} - 3\eta_{12})^2 + (3\eta_{21} - \eta_{03})^2,$$

$$\phi_4 = (\eta_{30} + \eta_{12})^2 + (\eta_{21} + \eta_{03})^2,$$

$$\phi_5 = (\eta_{30} - 3\eta_{12})(\eta_{30} + \eta_{12})\left[(\eta_{30} - \eta_{12})^2 - 3(\eta_{21} + \eta_{03})^2\right]$$
$$+ (3\eta_{21} - \eta_{03})(\eta_{21} + \eta_{03})\left[3(\eta_{30} + \eta_{12})^2 - (\eta_{21} + \eta_{03})^2\right],$$

$$\phi_6 = (\eta_{20} - \eta_{02})\left[(\eta_{30} + \eta_{12})^2 - (\eta_{21} + \eta_{03})^2\right] + 4\eta_{11}(\eta_{30} + \eta_{12})(\eta_{21} + \eta_{03})$$

$$\phi_7 = (3\eta_{21} - \eta_{30})(\eta_{30} + \eta_{12})\left[(\eta_{30} + \eta_{12})^2 - 3(\eta_{21} + \eta_{03})^2\right]$$
$$+ (3\eta_{12} - \eta_{30})(\eta_{21} + \eta_{03})\left[\left(3(\eta_{30} + \eta_{12})^2 - (\eta_{21} + \eta_{03})^2\right)\right].$$

This set of moments is invariant to translation, rotation and scale change. The flowchart of feature extraction of the statistical moment method is depicted in Figure 8.

4.4 GDC Method: Gradient Direction Coding with Gray code

The method, called the GDC method, used here is the gray coding that is a 2-D method and designed to encode the gradient direction of each small 2-D palmprint image block in wavelet transform domain. The scale of the wavelet representation we select in this method is j=1, 2, and 3. The flowchart of feature extraction and encoding of the GDC method is depicted in Figure 9.

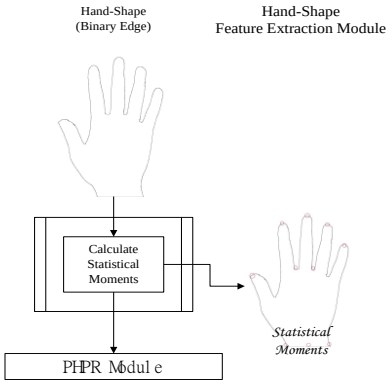

Figure 8 The flowchart of feature extraction of hand geometry image in the statistical moments method.

In order to reduce the code length of iris features and avoid affected by noise, we encode these features by using the Gray code concept, as shown in Figure 10. In the proposed gray code, the region of [0, 2π] is equally divided into eight intervals that each covers 45° and each interval is encoded by a 4-bit code. The codes corresponding to the adjacent intervals differ from only one bit, thus the Hamming distance between them is minimum. On the other hand, the codes corresponding to the interval which differ 180° are different by all of the four bits, thus the Hamming distance between them is maximum.

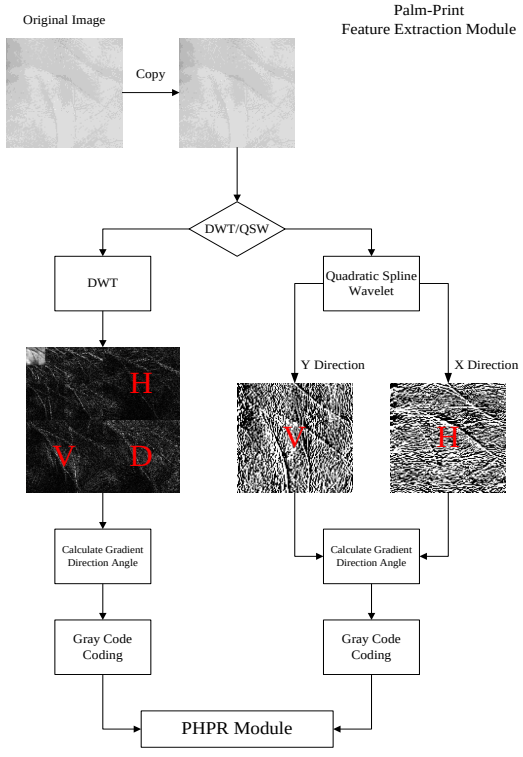

Figure 9 The flowchart of the feature extraction and encoding in the GDC method.

4.5 Recognition Module

In this module, the feature code vector extracted from the claimant hand image is compared against those of the enrolled feature code vectors in the PPC & SMV database we created. Here for simplicity, we adopt the mean vector as the prototype of each pattern class in the enrolment phase and utilize the minimum distance classifier to check the approach in the recognition phase [36]. First, we compute the Euclidean distance D between two hand geometry feature code vectors ϕ^t and ϕ^k, which is defined as

$$D(\phi^t,\phi^k)=\sqrt{\sum_{i=1}^{7}(\phi_i^t-\phi_i^k)^2}\ .$$

Second, we sort the closest distances to the ten classes. Finally, we compute the normalized Hamming distance between two palmprint feature code vectors h_1 and h_2, which is denoted as

$$HD(h_1,h_2)=\min\frac{\sum_{k=0}^{k=m}\sum_{l=0}^{l=n}h_1^A(k,l)\oplus h_2^A(k,l)}{m\times n},\ HD\in[0,1].$$

The HD minimum distance classifier is normalized to [0, 1].

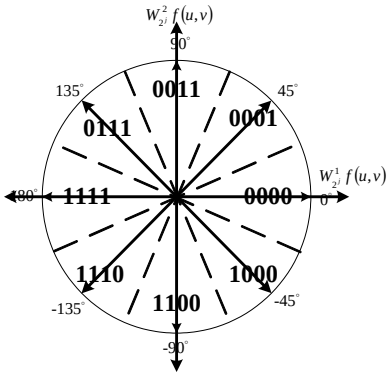

Figure 10 Encoding the features with Gray code.

5. EXPERIMENTAL RESULTS

To evaluate the performance of the proposed palmprint and hand geometry recognition system, we implemented and tested the proposed schemes on VIP-CC Laboratory's hand image database, built by Institute of Electrical Engineering, National Chi Nan University. It comprises 210 hand images captured from 30 different human (hence 30 classes). Each original hand image has a resolution of 1,280×960 with 24-bit color. For each hand, seven images are captured in two phases.

In an identification system, the performance can be measured in terms of three different factors:

(1) False Acceptance Rate (FAR): the probability of identifying an impostor as an enrolled user;

(2) False Rejection Rate (FRR): the probability of rejecting an enrolled user, as if he is an impostor;

(3) Equal Error Rate (EER): the value where the FAR and FRR rates are equal.

Figure 11 shows the plot of variation of FAR and FRR by selecting a proper distance threshold. When we set the thresholds to be 0.51, 0.47 and 0.42, the system obtains the recognition performances of about EER=5.83%, 3.33% and 1.67% using the QSW method with the levels 1~3. And when the FAR is set to be 0%, the system can obtain FRR=8.83%, 6.67% and 3.33% at a threshold of 0.32, 0.29 and 0.23 using the QSW method with the levels 1~3. The experimental results show that the proposed system performs well.

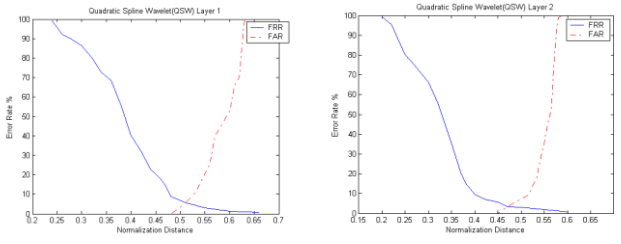

(a) Level-1 (b) Level-2

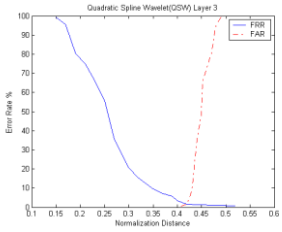

(c) Level-3.

Figure 11 The results of the QSW method.

Finally, we make a summary of the experimental results show in Table 1. It can be seen from in the results that the QSW method has a superior performance to the DWT method by comparing the EER and in the case of FAR=0% performance. On the other hand, the DWT method has a short palmprint code in our system and has a good performance.

Mode	FE Module	RA (%)	AA (%)	AF (%)	RF (%)
ERR	DWT -L1	7.50	92.50	7.50	92.50
	DWT- L2	5.00	95.00	5.00	95.00
	DWT- L3	8.83	91.17	8.83	91.17
	QSW-L1	5.83	94.17	5.83	94.17
	QSW-L2	3.33	96.67	3.33	96.67
	QSW-L3	1.67	98.33	1.67	98.33
FAR = 0%	DWT- L1	8.83	91.17	0	100
	DWT- L2	6.67	93.33	0	100
	DWT -L3	10.83	89.17	0	100
	QSW-L1	8.83	91.17	0	100
	QSW-L2	5.83	94.17	0	100
	QSW-L3	3.33	96.67	0	100

Table 1 Identification accuracy of the DWT and QSW methods.

6. CONCLUSION

In this paper, a personal verification system with palmprint and hand geometry recognition based on wavelet transform and statistical moments has been proposed. We used two different wavelet transform methods which including DWT and QSW, and invariant moments, in feature extraction module. All methods can obtain a good recognition rate. If the system sets FAR to be 0%, the recognition rates can approach more than 89%. In the QSW-L3 case, the proposed system has the best performance in 98.33%.

REFERENCES

[1] A. K. Jain, R. Bolle and S. Pankanti, *Biometrics: Personal Identification in Network Society*. Kluwer Academic Publishers, 1999.

[2] B. Miller, "Vital signs of identity," *IEEE Spectrum*, Feb, pp. 22-30. 1994.

[3] M. Golfarelli, D. Miao and D. Maltoni, "On the error-reject trade-off in biometric verification systems," *IEEE Trans. on Pattern Analysis and Machine Intelligence*, vol. 19, pp. 786-796, 1997.

[4] A. K. Jain, A. Ross and S. Pankanti, "A prototype hand geometry-based verification system," *Proc. of 2nd International Conference on Audio- and Video-based Biometric Person Authentication (AVBPA1999)*, pp. 166-171, 1999.

[5] A. K. Jain and N. Duta, "Deformable matching of hand shapes for user verification," *Proc. of International Conference on Image Processing*, 1999.

[6] R. Sanchez-Reillo, C. Sanchez-Avila and A. Gonzalez-Marcos, "Biometric identification through hand geometry measurements," *IEEE Trans. on Pattern Analysis and Machine Intelligence*, vol. 22, pp. 1168-1171, 2000.

[7] R. Sanchez-Reillo, "Hand geometry pattern recognition through Gaussian mixture modeling," *International Conference on Pattern Recognition*, vol. 2, pp. 937-940, 2000.

[8] A. Wong and P. Shi, "Peg-free hand geometry recognition using hierarchical geometry and shape matching," *Proc. of IAPR Workshop on Machine Vision Applications*, pp. 281-284, 2002.

[9] G. Zheng, T. E. Boult and C-J. Wang, "Projective invariant hand geometry: an overview," *Biometrics Symposium (BSYM)*, 2005.

[10] R. L. Zunkel, Hand geometry based verification, in: A. K. Jain, R. Bolle and S. Pankanti (eds.), *Biometric: Personal Identification in Network Society*, Kluwer Academic Publishers, pp. 87-101, 1999.

[11] R. H. Ernst, "Hand ID system," *US Patent No. 3576537*, 1971.

[12] D. P. Sidlauskas, "3D hand profile identification apparatus," *US Patent No. 4736203*, 1988.

[13] "HaSIS-A hand shape identification system," *http://www.csr.unibo.it/research/biolab/hand.htm*.

[14] W. Shu and D. Zhang, "Automated personal identification by palmprint," *Optical Engineering*, vol. 37, No. 8, pp. 2359-2362, 1998.

[15] D. Zhang and W. Shu, "Two novel characteristics in palmprint verification: datum point invariance and line feature matching," *Pattern Recognition*, vol. 32, pp. 691-702, 1999.

[16] N. Duta, A. K. Jain and K. V. Mardia, "Matching of palmprint," *Pattern Recognition Letters*, vol. 23, pp. 477-485, 2002.

[17] C.-C. Han, H.-L. Cheng, C.-L. Lin and K.-C. Fan, "Personal authentication using palm-print features," *Pattern Recognition*, vol. 36, pp. 371-381, 2003.

[18] D. Zhang, *Automated Biometrics---Technologies and Systems*, Kluwer Academic Publishers, 2000.

[19] Y.-H. Pang, A. T. B. Jin, D. N. C. Ling and H. F. San, "Palmprint verification with moments," Journal of WSCG, vol. 12, No. 1-3, 2003.

[20] Y.-H. Pang, A. T. B. Jin and D. N. C. Ling, "Palmprint authentication system using wavelet based pseudo Zernike moments features," *International Journal of the Computer, the Internet and Management*, vol. 13, No. 2, pp. 13-26, 2005.

[21] J. You, W. Li and D. Zhang, "Hierarchical palmprint identification via multiple feature extraction," *Pattern Recognition*, vol. 35, pp. 847-859, 2002.

[22] X. Wu, K. Wang and D. Zhang, "Fuzzy Directional Element Energy Feature (FDEEF) based palmprint identification," *International Conference on Pattern Recognition*, vol. 1, pp. 95-98, 2002.

[23] M. D. Jain, S. N. Pradeep and R. Balasubramanian, "Nearest neighbor vector based palmprint verification," *Proceeding of Visualization, Imaging and Image Processing*, 2005.

[24] W. Li, D. Zhang and Z. Xu, "Palmprint identification by Fourier transform," *International Journal of Pattern Recognition and Artificial Intelligence*, vol. 16, No. 4, pp. 417-432, 2002.

[25] A. Kumar and H. C. Shen, "Recognition of palmprints using wavelet-based features," *Proc. of International Conference on Systems and Cybernetics*, 2002.

[26] W. K. Kong, D. Zhang and W. Li, "Palmprint feature using 2-D Gabor filter," *Pattern Recognition*, vol. 36, pp. 2339-2347, 2003.

[27] D. Zhang, W. K. Kong, J. You and M. Wong, "Online palmprint identification," IEEE Trans. on *Pattern Analysis and Machine Intelligence*, vol. 25, No. 9, pp. 1041-1050, Sept. 2003.

[28] K. Liu, Y. Cheng and J. Yang, "Algebraic feature extraction for image recognition based on an optimal discriminant criterion," *Pattern Recognition*, vol. 26, pp. 903-911, 1993.

[29] R. O. Duda, O. E. Hart and D. G. Stork, *Pattern Classification*, John Wiley & Sons, Inc., 2001.

[30] G. Lu, D. Zhang and K. Wang, "Palmprint recognition using eigenpalms features," *Pattern Recognition Letters*, vol. 24, pp. 1463-1467, 2003.

[31] X. Wu, D. Zhang and K. Wang, "Fisherpalms based palmprint recognition," *Pattern Recognition Letters*, vol. 24, pp. 2829-2838, 2003.

[32] T. Connie, A. Teoh, M. Goh and D. Ngo, "Palmprint recognition with PCA and ICA," *Proc. of Conference on Image and Vision Computing*, New Zealand, pp. 227-232, Nov. 2003.

[33] NEC Automatic Palmprint Identification System--- *http://www.nectech.com/afis/ download/PalmprintDtsht.q.pdf*, 2003.

[34] C. C. Han, P. C. Chang and C. C. Hsu, "Personal identification using hand geometry and palmprint," *Proc. of Fourth Asian Conference on Computer Vision (ACCV)*, pp. 747-752, 2000.

[35] A. Kumar, D. C. M. Wong, H. C. Shen and A. K. Jain, "Personal verification using palmprint and hand geometry biometrics," *Proc. of 4th International Conference on Audio- and Video-based Biometric Person Authentication (AVBPA2003)*, 2003.

[36] R. C. Gonzalez and R. E. Woods, *Digital Image Processing*, 2nd Edition, Prentice-Hall, New Jersey, 2002.

[37] J. R. Parker, *Algorithms for Image Processing and Computer Vision*, John Wiley & Sons, 1996.

[38] S. Mallat, *A Wavelet Tour of Signal Processing*, 2nd Edition, Academic Press, San Diego, 2001.

[39] J. Canny, "A computational approach to edge detection," *IEEE Trans. on Pattern Analysis and Machine Intelligence*, vol. 8, No. 6, pp. 679-698, 1986.

[40] S. Mallat and S. Zhong, "Characterization of signals from multiscale edge," *IEEE Trans. on Pattern Analysis and Machine Intelligence*, vol. 14, No. 7, pp. 710-732, 1992.

[41] Y. Y. Tang *et al*., *Wavelet Theory and Its Application to Pattern Recognition*, World Scientific, Singapore, 2000.